

EVIDENCE FOR STELLAR CHROMOSPHERES PRESENTED BY ULTRAVIOLET OBSERVATIONS OF THE SUN AND STARS

Lowell Doherty

*Space Astronomy Laboratory, Washburn Observatory
University of Wisconsin*

I would like to describe observations of emission lines in stellar sources, in the ultraviolet region of the spectrum not accessible to ground observation. As we have heard, the interpretation of emission lines may involve both geometrical and temperature effects, so that the occurrence of emission lines does not constitute *prima facie* evidence for chromospheres. On the other hand, we have not yet, at this conference, formulated a definition of a chromosphere that excludes any particular category of stellar emission-line objects.

In principle, information on chromospheric structure is also contained in the continuum. However, the measurement of accurate spectral energy distributions depends on the very difficult process of ultraviolet photometric calibration. This work is continuing both at Goddard and the University of Wisconsin. I will not discuss continuum observations here. Wilson and Boksenberg (1969) have extensively reviewed instrumentation and results in ultraviolet astronomy up to 1969. The most recent results will be discussed in a forthcoming review article by Bless and Code (1972).

Observations of ultraviolet emission lines are as yet confined to a few stars, and I will try to describe most of these observations briefly, with emphasis on work done since Wilson and Boksenberg (1969). Let us begin with the stars of earliest spectral type. The spectra of Wolf-Rayet stars are sprinkled with the resonance lines of C, N, and Si, excited lines of these elements and of He II. Figure II-1 shows OAO photoelectric scans of two Wolf-Rayet stars. The short-wavelength segments of these scans ($\lambda < 1800\text{\AA}$) have a resolution of about 12 \AA , while the long-wavelength segments, made with a different spectrometer, have a resolution of about 25 \AA . Even at the low resolution of these scans, P Cyg profiles are evident in a number of lines, especially the resonance doublets N V $\lambda 1240$ and C IV $\lambda 1550$. In HD 50896 (WN5), $\lambda 1496$ and $\lambda 1719$ of N V and $\lambda 1640$ of He II are strong, as are other longer-wavelength lines of N and He. In γ Vel (WC7) the C spectrum is well developed. γ Vel has also been observed at 10 \AA resolution (Stecher 1970) and photographically at higher resolution (Wilson and Boksenberg 1969). L. Smith (1972) has interpreted the strengths of ultraviolet C, N, and O lines in HD 50896 to

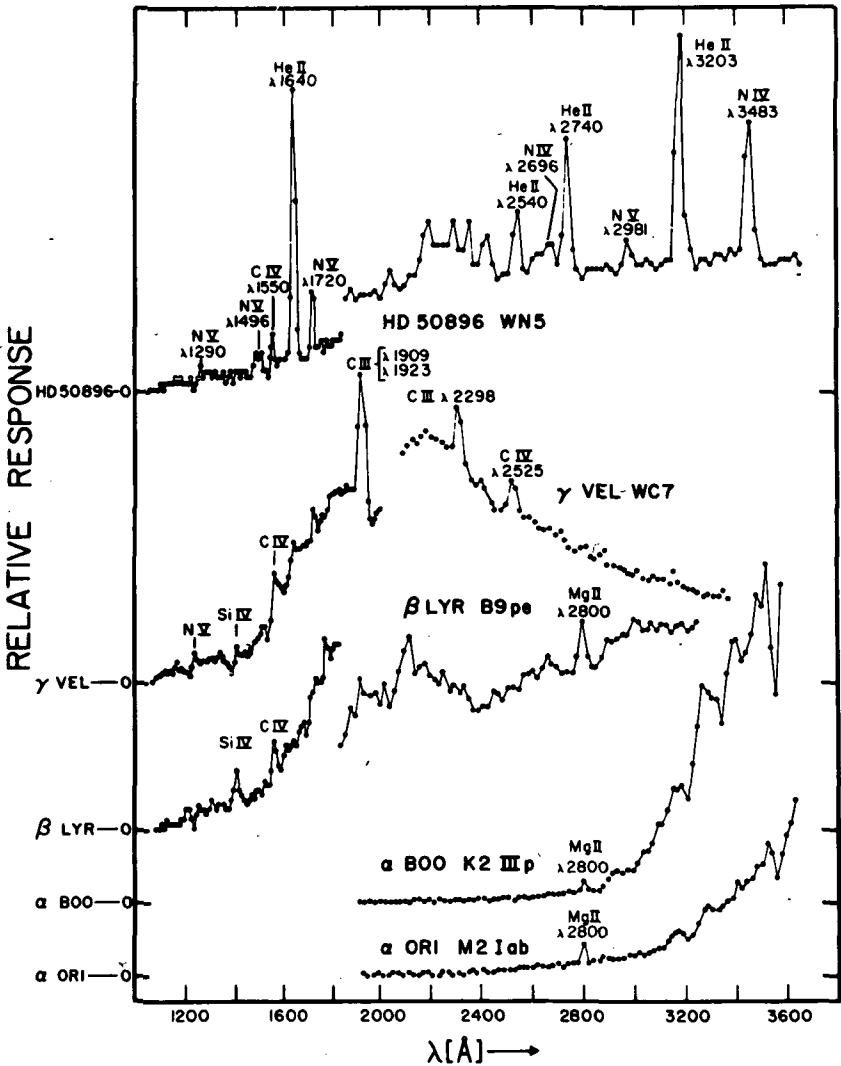


Figure II-1 OAO scans of selected stars. Short-wavelength segments have a resolution of approximately 12 \AA , and the long-wavelength segments 25 \AA .

mean that selective excitation processes are unimportant, with the implication that differences between WN and WC spectra reflect real abundance differences.

Among O and B stars, emission has been observed in 6 Orion stars of spectral type O9 to B2 and luminosity class I to III, and in ζ Pup (O5f) and ξ Per (O7). Analysis of 2\AA resolution photographic spectra of 5 of the Orion stars (Morton, Jenkins and Bohlin 1968) established that

expansion velocities of some 1500 km/sec exist in the envelopes of these stars, and that there is a velocity gradient for the ultraviolet lines. The highest velocities were obtained from the absorption components of the P Cyg profiles of resonance lines of Si III, Si IV, C IV, and N V. For $\lambda 1175$ of C III, velocities were between 500 and 1000 km/sec, substantially lower than for the resonance lines. Since $\lambda 1175$ arises from a 6 eV excited level of the resonance triplet and is presumably formed closer to the stellar surface, the velocity of expansion must increase outward. Later A. Smith (1970) and Carruthers (1971), with resolution close to 1 \AA , obtained $\lambda 1175$ velocities near 1600 km/sec in the two very hot stars ζ Pup and ξ Per. However, as Carruthers points out, there is the possibility of blending of the C III lines with N IV $\lambda 1169$.

A. Smith (1970) recorded the spectrum of ζ Pup nearly to the Lyman limit and found the resonance lines of O VI and S VI, which had previously been observed only in the solar spectrum. S VI $\lambda 933$ has a velocity of 1380 km/sec, while O VI $\lambda 1030$ and the $\lambda 990$ resonance line of N III have velocities close to 1800 km/sec, which is typical of the resonance lines at longer wavelengths in ζ Pup. The more recent observations also suggest a greater range of velocities. Carruthers (1971) found 2650 km/sec for N V $\lambda 1240$ in ξ Per, while A. Smith (1970) determined the very low value of 150 km/sec for the excited $\lambda 1340$ line of O IV.

A number of emission lines in ζ Pup, e.g. N V $\lambda 1240$, Si IV $\lambda 1400$ and C IV $\lambda 1550$, are sufficiently strong to be detected in OAO scans. The Si IV and C IV lines have also been seen in ζ Ori (09.5 Ib) and κ Ori (B0.5 Ia), and Si IV $\lambda 1400$ in the 4th magnitude 09.5 supergiant α Cam.

Emission lines have not been found in B dwarfs. For the bright Be star γ Cas, Bohlin (1970) identified the C IV $\lambda 1550$ line as P Cyg type, but absorption features of other resonance lines such as Si III $\lambda 1206$ and Si IV $\lambda 1400$ have their expected wavelengths and are labelled photospheric. Between the excited N IV $\lambda 1718$ line and 2100 \AA the spectrum of γ Cas at 2 \AA resolution is rather featureless. β Lyrae (B9 pe) shows an emission spectrum which probably arises in a large cloud surrounding the component stars (Houck 1972). A sample OAO scan is shown in Figure 1. In addition to some of the far ultraviolet resonance lines we have mentioned, Mg II $\lambda 2800$ emission is also apparent in γ Lyrae.

Although of less interest, perhaps, for the problem of stellar chromospheres, ultraviolet observations exist for Nova Serpentis 1970 (Code 1972). OAO scans of the $\lambda > 2000$ \AA region indicate a changing complex spectrum whose features cannot be easily identified at low resolution.

Among normal stars of later type, the sun, if located a few parsecs away, and viewed with spectral resolution comparable to that used in present

stellar rocket experiments, could be recognized as a star with a chromosphere. Low flux levels would make such observations difficult, however. Shortward of Mg II $\lambda 2800$, the ultraviolet emission spectrum of the Sun does not appear until Si II $\lambda 1810$, and C IV $\lambda 1550$ is the first indication of fairly high temperatures. Observation of the corona would be limited to O VI $\lambda 1030$, since interstellar hydrogen would obliterate the spectrum below the Lyman limit. The solar Lyman lines would also be strongly absorbed.

OAo scans are available for a number of bright stars of spectral type G and later. For such cool stars, data can be obtained only with the long wavelength spectrometer, and in most cases the scans are useful only for $\lambda > 2500$ Å approximately. Figure 1 includes scans of α Boo (K2 III) and α Ori (M2 Iab), which show how rapidly the flux decreases toward shorter wavelengths. Mg II $\lambda 2800$ is clearly in emission in these stars. No features, either in absorption or emission, have been identified for $\lambda < 2800$ Å in OAO scans of these or other K and M stars. Even where counting rates are relatively large, only gross features of the spectrum are apparent at 25 Å resolution. Figure II-2 shows part of an OAO scan of α Cen (G2 V). One OAO (reduced) count equals 64 photomultiplier events. For comparison, the solar spectrum has been smeared to a resolution of 20 Å and normalized to the stellar scan at 2900 Å. The major features of this spectrum are Mg I $\lambda 2852$, Mg II $\lambda 2800$, and the group of Fe II lines near $\lambda 2740$. There is no indication of solar Mg II emission at this resolution. The OAO spectrometer is stepped at intervals of 20 Å, and, as Figure II-2 shows, it would be difficult to interpolate accurately between the discrete data points without the aid of the known solar spectrum. Moreover, scanner wavelengths are normally known only to about ± 10 Å. Thus OAO scans of late-type stars must be interpreted with caution.

Figure II-3 shows the changing character of the spectrum with later spectral type for the region $\lambda > 2800$ Å. Ordinate scales are different for each of the four stars. The location of prominent features of the solar spectrum are marked here for comparison. The scans at least appear to form a fairly smooth sequence with differences attributable to differences in excitation. One noteworthy feature of α Ori is the bump near 3180 Å which is due, presumably, to Fe II emission which Weymann discussed a number of years ago (1962). It is not known where these lines are formed. Profiles of one group of lines are similar to solar Ca II K, but complex velocity fields make the interpretation of these lines difficult. I believe Ann Boesgaard will report on some recent observations of these lines later today. I would like to point out that OAO scans of α Ori set upper limits to the flux in several Fe II multiplets whose upper levels are common to the multiplets that produce the near ultraviolet emission (Doherty 1972).

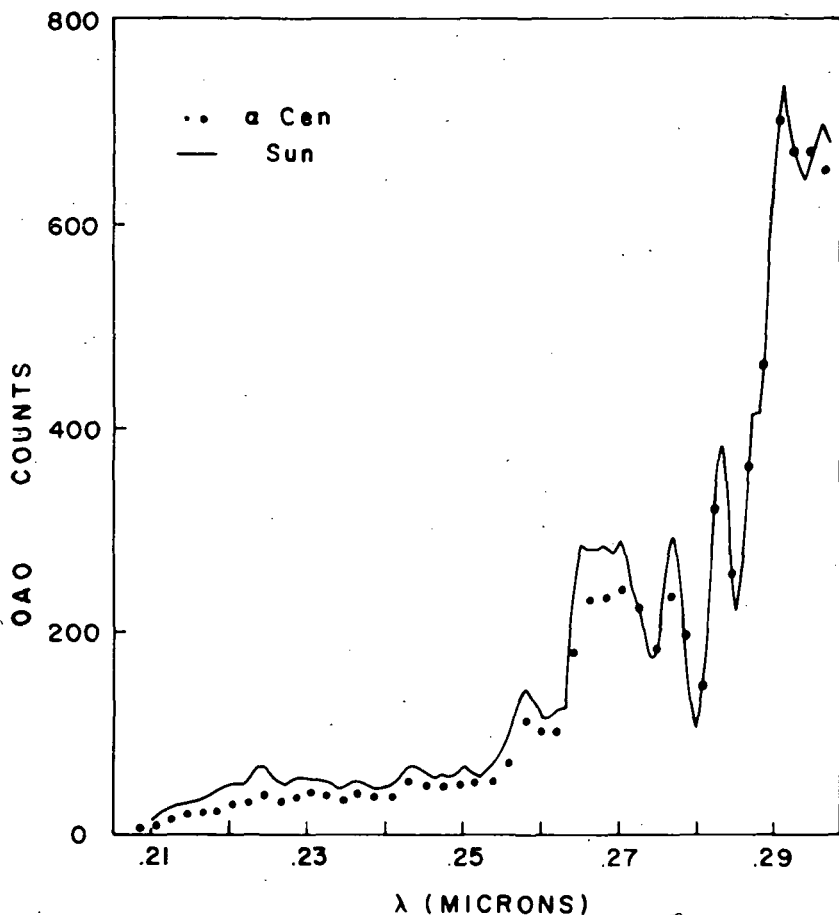


Figure II-2 OAO scan of α Cen compared with the solar spectrum smeared to a resolution of 20 \AA and normalized to the scan at 2900 \AA .

For all very cool, bright stars Mg II emission is clearly seen in OAO scans. Figure II-4 illustrates the 2800 \AA region in several class III giants. Dots indicate OAO (reduced) counts measured at discrete intervals of 20 \AA . Approximate sky background has been subtracted. Exact wavelength registration cannot be determined, but, 2800 \AA does fall between the 5th and 6th channels, as counted from the left. Figure II-5 shows the Mg II region for supergiants. Only the class I stars definitely show emission here. Although Mg II emission fluxes can be determined only approximately from the OAO scans, there is evidence from stars with the strongest emission that the ratio of Mg-II to Ca II K emission flux does not differ greatly from star to star. Figure II-6 compares estimated Mg II

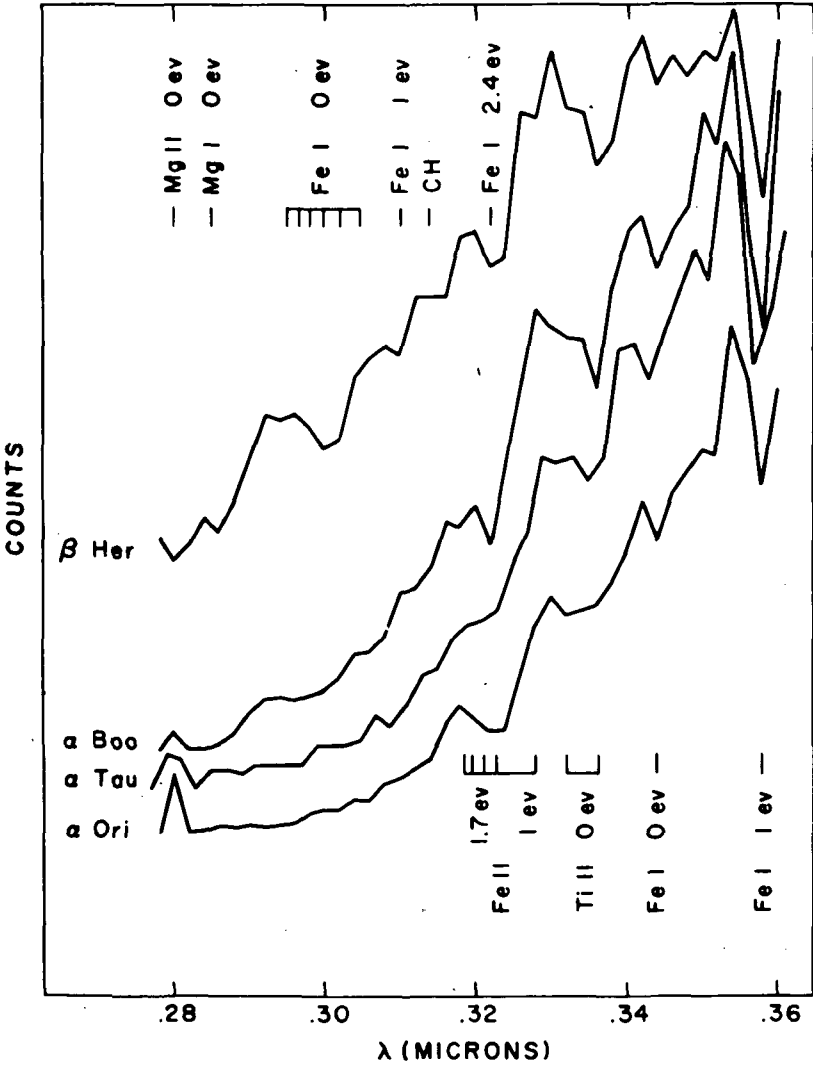


Figure II-3 Changes in ultraviolet spectral features with different spectral type at approximately 25 \AA resolution. Ordinate scales are arbitrary. Principal features of the solar spectrum are indicated. β Her, G8 III; α Boo, K2 III; α Tau, K5 III; α Ori, M2 Iab.

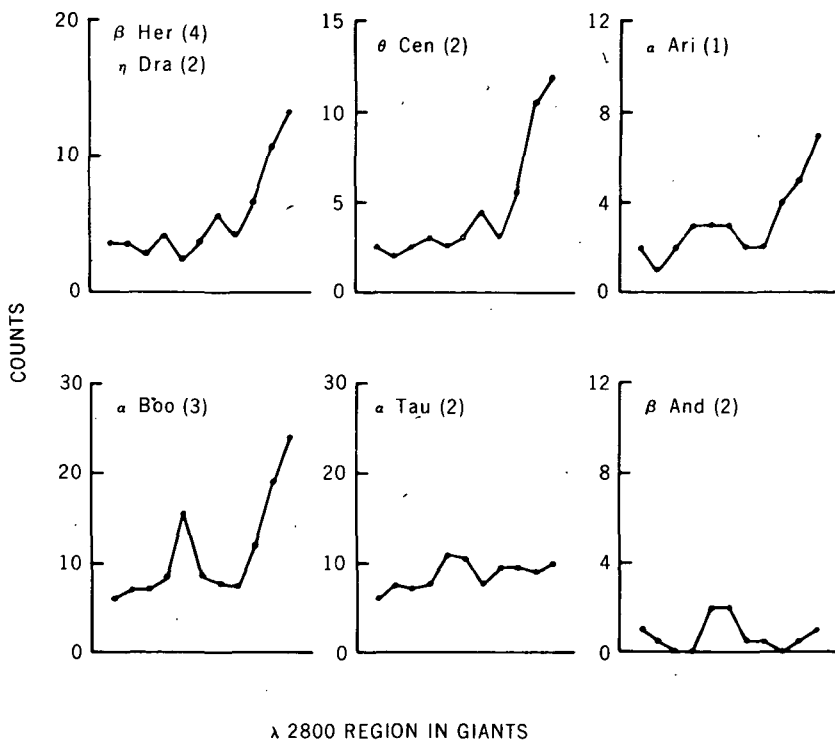
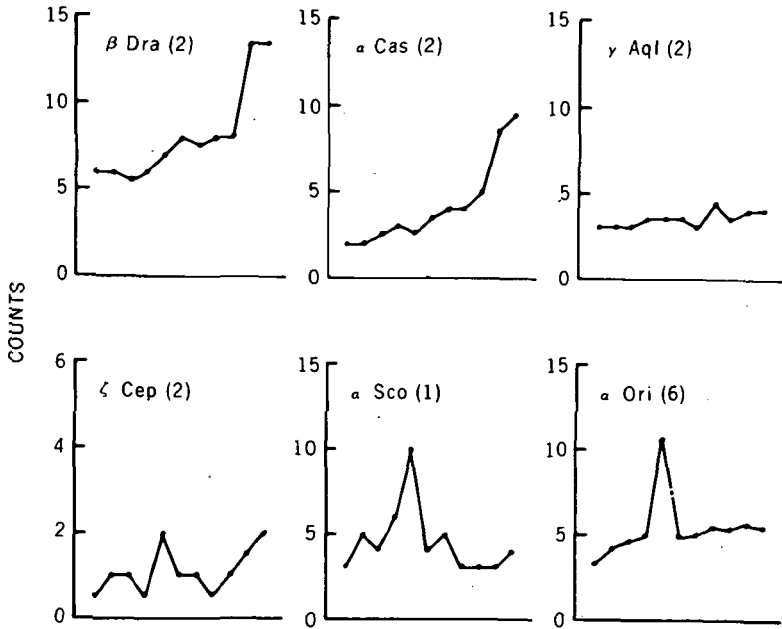


Figure II-4 Spectra of selected G-M giant stars in the 2800 Å region. These averaged OAO scan segments cover 220 Å, with the position of $\lambda 2800$ falling between the 5th and 6th channel as counted from the left.

emission. counts for 8 stars with IW, a measure of the Ca II K emission flux observed at the earth (Doherty 1972).

Vertical bars indicate the limiting values for the Mg II counts that must be assigned as a result of the uncertainty in the strength of the underlying absorption feature. These stars are giants and supergiants of spectral type K2-M2. Within the errors of measurement it is possible that the ratio Mg II/Ca II K is the same for all of these stars. The solar symbol shows the position the Sun would occupy if its visual magnitude were zero. The method of calculating IW does not attempt to subtract the underlying absorption profile of the K line. This does not affect the stellar values appreciably, but the solar value of IW in Figure II-6 represents the total flux emitted in the wavelength band that includes the K emission core and not the net emission. Thus the significance of the approximate agreement between the ratio for the Sun and stars with strong K emission is not immediately apparent.



λ 2800 REGION IN SUPERGIANTS

Figure II-5 Spectra of selected G-M supergiant stars in the 2800 Å region.

Recently, Kondo, Modisette and Giuli (1971) have obtained high-resolution ($1/2 \text{ \AA}$) photoelectric scans of the 2800 Å region in 5 stars covering a wide range of spectral type. The observations were made from a balloon. They find that α Ori has doubly-reversed Mg II cores, qualitatively similar to the profiles of the solar lines. The only other cool star for which Mg II has been observed with better than OAO resolution is Arcturus. At a resolution of 7 \AA Mg II appears as a single emission line in this star (Kondo 1972). Arcturus has also been observed in the far ultraviolet by Moos and Rottman (1971) who report the measurement of emission in Lyman α and a line which is probably $\lambda 1304$ of OI.

It is exciting to consider the prospect of having further, more detailed observations of the ultraviolet spectra of stars that we expect to have chromospheres similar to the Sun's. Such observations will, however, be relatively difficult and costly, due to the very low fluxes that must be measured. If we look at the characteristics of the rocket spectrographs (both photographic and electronographic) that have been used to obtain 1

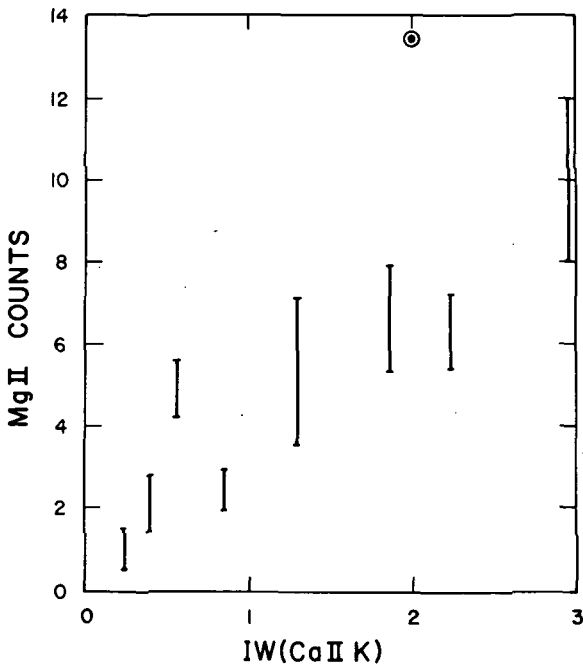


Figure II-6 Mg II $\lambda 2800$ emission (OAO reduced counts) vs. IW, a measure of Ca II K emission flux at the Earth. The Sun is shown as it would appear if it were a V=0 star measured in the same way.

\AA resolution spectra of O and B stars, these instruments have, on the average, a product of collecting area times exposure equal to roughly $1500 \text{ cm}^2 \text{ sec}$. To obtain the same kind of data for cooler stars of the same visual magnitude, the aperture or the observing time must be larger. In the far ultraviolet, the increase can be enormous. Figure II-7 is a color-color diagram obtained from OAO wide-band filter observations at 1700 \AA . Relative to the visual, the 1700 \AA flux of stars varies by a factor of almost 10^4 from type O to the coolest stars shown, which have slightly earlier spectral types than the Sun. Increases in collecting area and exposure of this magnitude cannot be accommodated in rocket experiments. Thus different techniques must be considered. For example, completely photoelectronic recording can increase the instrumental sensitivity. At present, however, the gain is fully realized only by observation of one spectral band in one object (with one photometer). Continuing development of electronic image intensification and recording systems promises eventually to help this problem by making possible essentially

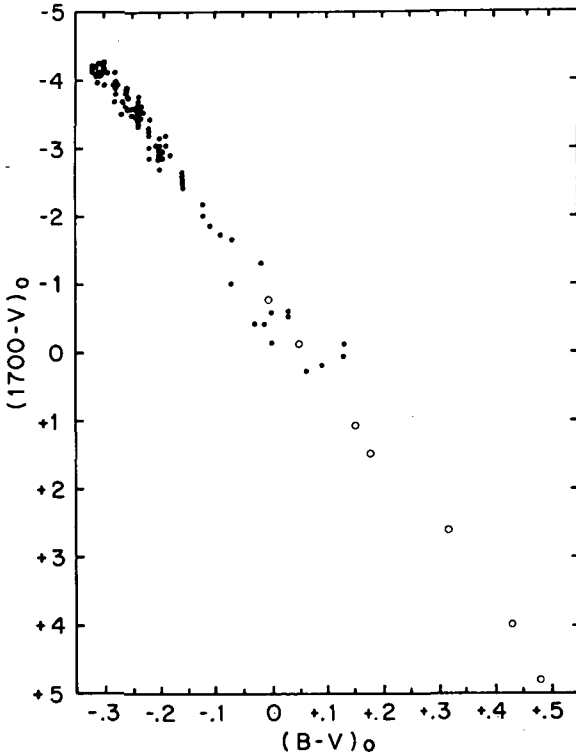


Figure II-7 Stellar $\lambda 1700 - V$ color vs. $B - V$ with 1700 \AA wide-band photometry from OAO.

simultaneous observation of many image elements. Nevertheless, different, generally more restrictive kinds of observations will be necessary for cool stars.

It is possible that the already large factor of 10^4 decrease in flux we have seen in Figure 6 will not become greater for certain observations made at wavelengths shorter than 1700 \AA or for cooler stars. In the Sun the strongest chromospheric lines between 1700 \AA and the Lyman limit produce about the same photon flux as 1 \AA of the continuum near 1700 \AA . If stars of later type than the Sun have chromospheric temperatures more nearly like the solar chromosphere, then the detection of their strongest emission lines might be possible with the same effort required to observe solar-type stars, for which the factor 10^4 applies roughly to all strong lines.

Given the much greater difficulty of obtaining ultraviolet data for cool stars, perhaps some theoretical work might be directed toward the question of which specific ultraviolet measurements would be most helpful in understanding the nature of stellar chromospheres. Guidelines of this sort could prove very useful for the efficient selection and design of future ultraviolet experiments.

Preparation of this paper was supported, in part, by NASA NAS 5-1348 contract.

REFERENCES

- Bless, R.C. and Code, A.D. 1972, *Ann. Rev. Astron. Astrophys.*, in press.
 Bohlin, R.C. 1970, *Astrophys. J.*, **162**, 571.
 Carruthers, G.R. 1971, *Astrophys. J.*, **166**, 349.
 Code, A.D. 1972, in *Sci. Results of OAO-2*, ed. A.D. Code (Washington: U.S. Government Printing Office), in press.
 Doherty, L.R. 1972, *ibid.*
 Houck, T.E. 1972, *ibid.*
 Kondo, Y. 1972, *Astrophys. J.*, **171**, 605.
 Kondo, Y., Modisette, J.L., and Giuli, R.T. 1971, paper presented at 136th meeting of A.A.S.
 Moos, H.W., and Rottman, G.J. 1971, *ibid.*
 Morton, D.C., Jenkins, E.B., and Bohlin, R.C. 1968, *Astrophys. J.*, **154**, 661.
 Smith, A.M. 1970, *Astrophys. J.*, **160**, 595.
 Smith, L.F. 1972, in *Sci. Results of OAO-2*, ed A.D. Code (Washington: U.S. Government Printing Office), in press.
 Stecher, T.P. 1970, *Astrophys. J.*, **159**, 543.
 Weyman, R. 1962, *Astrophys. J.*, **136**, 844.
 Wilson, R. and Boksenberg, A. 1969, *Ann. Rev. Astron. Astrophys.*, **7**, 421.

DISCUSSION FOLLOWING TALKS BY PRADERIE AND DOHERTY

Kuhi — Now I'd like to call on Rottman to give you a summary of his uv spectral work on Arcturus.

Rottman — I would like to discuss an ultraviolet spectrum of Arcturus obtained from a sounding rocket flight. This experiment was a sequel to one which identified the Ly α emission as reported in *Ap. J.* **165**, 661, 1971. In the present experiment, definite emission lines were observed in the spectral region 1200 Å to 1900 Å. It is expected that such

emission lines will give unambiguous evidence of the existence of and detailed information on chromospheric type layers. This work will be published by Warren Moos and myself.

Kuhi – I'd like for Kondo to present his work on high resolution scans of the Mg II resonance doublet in late type stars.

Kondo – This work was done in association with Tom Giuli and A.E. Rydgren of the NASA Manned Spacecraft Center and Jerry Modisette of Houston Baptist College. We report the initial results of a balloon-borne experiment designed to investigate emission of the Mg II resonance doublet in stars. The Mg II resonance doublet at 2795.5 Å and 2802.7 Å ($3s\ 2S - 3p\ 2P^o$) is the ultraviolet magnesium counterpart of the Ca II resonance doublet at 3933.7 Å and 3968.5 Å ($4s\ 2S - 4p\ 2P^o$). For certain spectral type stars the Ca II doublet has been observed in emission, which is believed to indicate chromospheric activity in these stars.

The Earth's atmosphere is opaque to radiation at 2800 Å, and until recently the Mg II doublet emission had been observed only in the solar spectrum, by means of rocket-borne and satellite payloads. Comparison of the Ca II and Mg II emission in the solar spectrum indicates that the latter is by far the more distinct and prominent of the two.

There are several theoretical reasons why the Mg II emission should be more prominent than the Ca II emission, at least for certain spectral types. First, the cosmic abundance of magnesium is about 17 times greater than that of calcium (Allen 1963). Second, the ionization and excitation potentials of magnesium and calcium are such that in A and F stars, the Mg II resonance lines are nearer to their maximum strength than are the Ca II resonance lines. Thus, for these stars one expects deeper and wider absorption lines for Mg II than for Ca II, which makes weak emission in the line bottom easier to detect. Third, for stars of spectral type later than A, the continuum level of 2800 Å is lower than at 3950 Å, facilitating detection of any weak emission. The Ca II doublet emission becomes difficult to observe in stars earlier than mid-F, and one of the objectives of this experiment is to determine whether the difficulty is due to observational limitation or to the disappearance of the mechanism responsible for the chromospheric emission. The other objective of this experiment is to survey the behavior of the Mg II resonance doublet in stars of various spectral types.

Recent low resolution UV spectrophotometry from OAO-2 (Doherty, 1971) and from a rocket (Kondo 1972) show Mg II doublet in unresolved emission for stars later than K2.

The current experiment was conceived to scan the Mg II doublet with spectral resolution of at least 0.5 Å for emissions anticipated for F-type dwarfs brighter than $m_v \approx 5$. It was felt that the 0.5 Å resolution would be required to unequivocally detect weak emission and also to study the detailed structure of stronger emission lines. The 0.5 Å resolution is a compromise between high resolution and available observing time. Current operational balloons can carry a sizeable telescope to altitudes approximating 40 km and can maintain those altitudes for an entire night. At these altitudes the atmospheric extinction for λ 2800 radiation is approximately 50% (Goldberg 1954), so one can expect balloon payloads to have decided advantages over rocket payloads for observations in this wavelength range.

Our payload consists of a 40 cm Cassegrain telescope with an Ebert-Fastie spectrometer, a three-stage star acquisition and tracking system, command and telemetry electronics, and structural components. Figure II-8 is a drawing of the assembled payload. A sketch of the instrument portion of the payload is shown in Figure II-9.

For acquisition of a target star, the telescope is pointed to within $1^\circ.5$ of the star in azimuth by referencing a two-element magnetometer to the horizontal component of the Earth's magnetic field. The telescope is pointed to within $0^\circ.5$ of the star in elevation by means of a position-sensing potentiometer referenced to local vertical. The platform star tracker acquires and centers the target star, which need not be the brightest star in the 1° by 3° field of view of this star tracker. This star is then tracked by the platform star tracker with an accuracy of ≈ 1 arc minute.

A dichroic filter located behind the primary telescope mirror reflects into the spectrometer the light from the star which is in a narrow band of wavelengths centered at 2800 Å. The visible light from the star is transmitted through the dichroic filter to an image position sensor. Position signals from this sensor are used to control the movable secondary mirror to maintain a fine-pointing accuracy of ± 1 arc seconds. The spectrometer grating has 2160 lines per mm and gives a second-order spectrum with a dispersion of 3.3 Å mm^{-1} . The detector for the spectrometer is an ITT F4012 image dissector tube with a $\frac{1}{4}$ Å "slit". The spectrum is scanned repetitively in $\frac{1}{4}$ Å steps with scan lengths of 4 Å, 24 Å or 50 Å. The appropriate scan length is chosen in real time and placed anywhere in the spectral range 2775 to 2825 Å by command from the ground. For further details regarding the payload and instrument, see Kondo et al. (1972), Gibsón et al. (1972) and Wells, Bottema and Ray (1972).

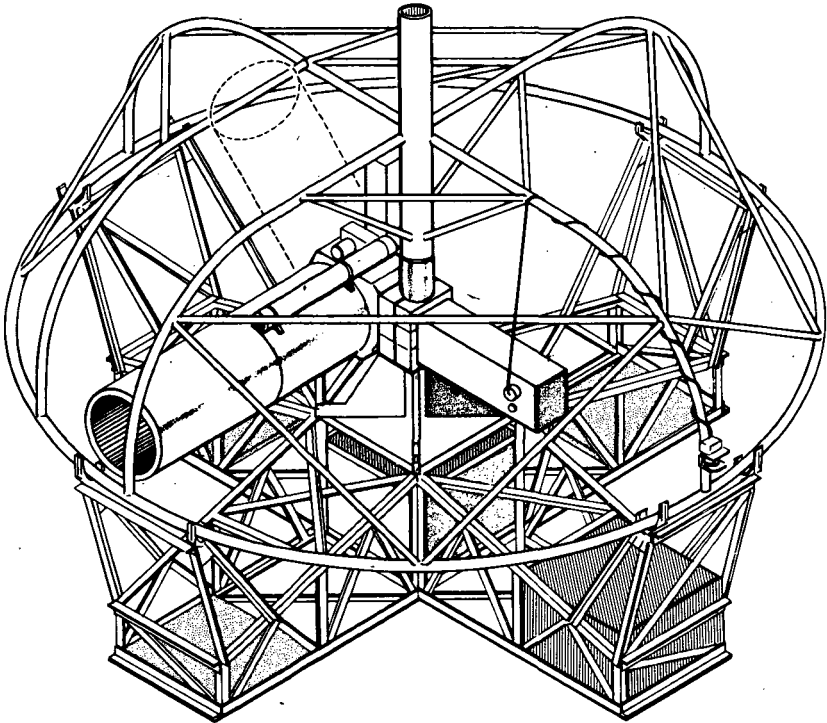


Figure II-8 Balloon-borne ultraviolet stellar telescope-spectrometer payload.

The payload is carried to an altitude of 40 km by a 430,000 m³ polyethylene single cell balloon. Observations are begun after payload sunset and continue until payload sunrise or until the payload drifts out of telemetry range (600 - 650 km from the ground station). The zenith obscuration at float altitude due to the balloon has a radius of 27°. The ground station at the launch site maintains continuous telemetry and command communication with the payload.

For target acquisition, it is necessary to provide the elevation and azimuth angles of the star relative to the payload's local vertical and magnetic north respectively. The latitude and longitude of the payload are monitored by means of the DOD Omega navigation system. The necessary calculations for target acquisition are performed in the ground station using a desk-top digital computer while observing another star. Normally, less than ten minutes are required to perform the calculations, transmit the commands and acquire the target star.

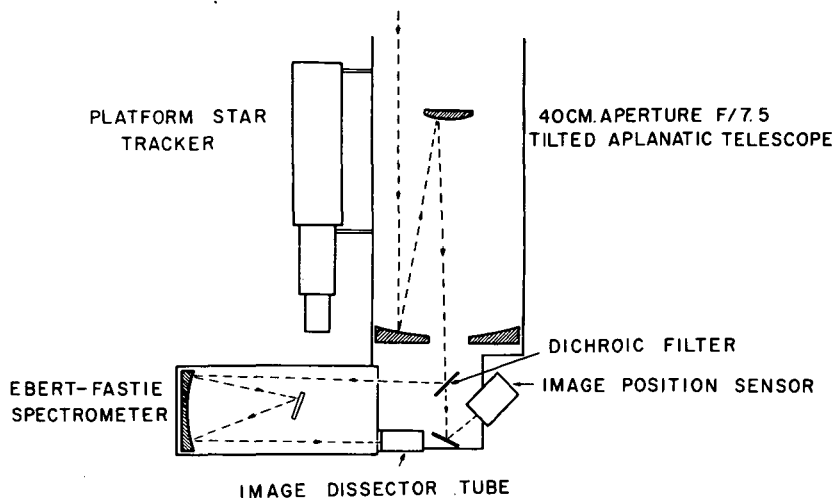


Figure II-9 Schematic telescope and spectrometer layout.

Once a target star is acquired, the scanning of the spectrum is begun and the data are telemetered to the ground station. The accumulated spectrum is displayed on a large oscilloscope so that the investigators can watch the counts build up, and the data are simultaneously recorded on magnetic tape for subsequent analysis. The oscilloscope data display allows the investigators to make real-time decisions regarding scan mode and length of observing time for each star.

Our raw data were in the form of counts per 50 milliseconds per $\frac{1}{4}$ Å channel. The magnetic tapes containing the data were analyzed to separate and accumulate the data for each star and to give the wavelength calibration and background count information. Using in-flight scans of an on-board wavelength reference lamp, we have calibrated our wavelength scales to an accuracy of $\pm \frac{1}{4}$ Å. Corrections for the Earth's orbital motion have been applied to reduce the observed wavelength scales to the Sun. No corrections for sky background and dark count have been made, since with the possible exception of the continuum of α Ori, they were negligible compared with the stellar flux.

From laboratory measurements and the analysis of in-flight wavelength reference line profiles, we have determined our resolution to be between 0.25 and 0.5 Å. Except as noted for γ Lyr, our data are presented in the form of observed counts per $\frac{1}{4}$ Å channel. The statistical uncertainty of each data point is the square root of the plotted value.

For the β Lyr data, an alternate approach was made to the error analysis, by generating Monte Carlo simulations of the spectrum taking into account both counting statistics and smearing in wavelength. The results with regard to identification of features were not significantly different from the conclusions indicated by the error bars in Figure II-10.

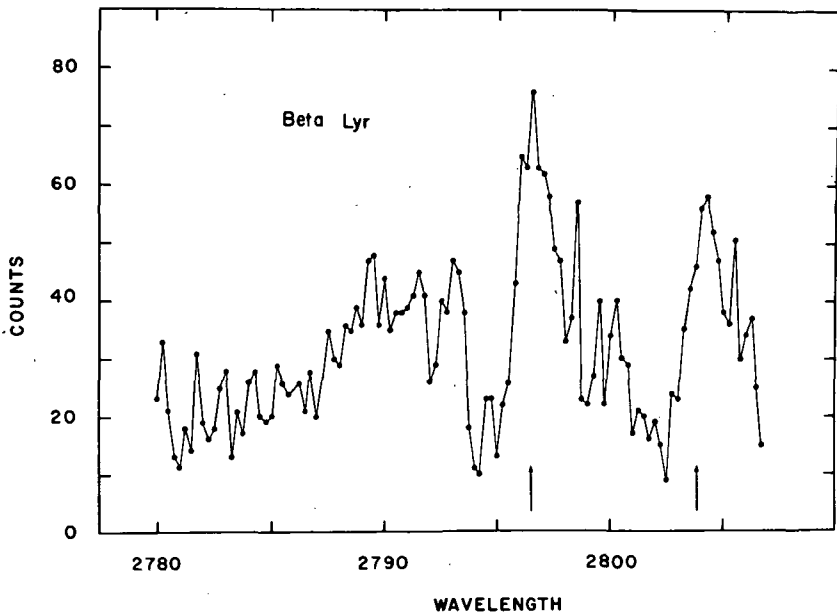


Figure II-10 Observation of the Mg II lines in β Lyr on 1971 June 6/7. The arrows indicate the Mg II line centers at the radial velocity of the B-star component at the time of observation.

We have thus far observed β Lyr, γ Lyr, β Cas, α CMi and α Ori. The first two were observed on the night of 1971 June 6/7, and the latter three were observed on the night of 1971 October 7/8.

β Lyr (*Bpe*, $m_v = 3.7v$) — The well-known eclipsing binary β Lyr was observed near 5^h UT on 1971 June 7. The presence of numerous emission features in the visible spectrum of β Lyr suggested that it would be a likely candidate for interesting spectral features involving the Mg II resonance doublet. This was borne out by our observations. One representative scan of β Lyr is shown in Figure 3. This shows broad overlapping emission features with deep absorption on the short-wavelength sides of the emission peaks. The line profiles are similar to the profiles of the emission lines in the visible spectrum of this star.

Using the ephemeris of Wood and Forbes (1963), we compute the phase of our observation to be OP.89. The radial velocity curve of Abt (1962)

gives a radial velocity of $+120 \text{ km sec}^{-1}$ for the B-star component at the phase of our observation. The line centers of the Mg II doublet in the B-star are near the tops of the emission peaks. The two absorption features are about 2 \AA or 200 km sec^{-1} in width. Abt determined the γ -velocity of the system to be $-19.5 \text{ km sec}^{-1}$. The line centers at the γ -velocity of the system are located in the deep absorption features.

We note that the emission spikes longward of the two emission peaks are statistically significant and are displaced equal amounts from the B star line centers. We obtained three other 50 \AA scans of $\beta \text{ Lyr}$ along with several partial scans. Intercomparison of this data suggests that there were significant changes in the emission portions of the features on a time scale of tens of minutes.

$\gamma \text{ Lyr}$ (B9III, $m_v = 3.3$) — We observed $\gamma \text{ Lyr}$ briefly during the first flight to confirm the accuracy of the pointing system of the payload. In the scan mode used to observe $\gamma \text{ Lyr}$, the time required to obtain 8 counts per $\frac{1}{4} \text{ \AA}$ channel was measured. Because of the low accuracy of this data, we have averaged this data over $\frac{1}{2} \text{ \AA}$ intervals. These data points have been converted for display purposes to the number of counts which would have been observed in 3.2 seconds per $\frac{1}{4} \text{ \AA}$ channel. The resulting scan of $\gamma \text{ Lyr}$ is shown in Figure II-11. The statistical uncertainty of each plotted point is 25% of the plotted value.

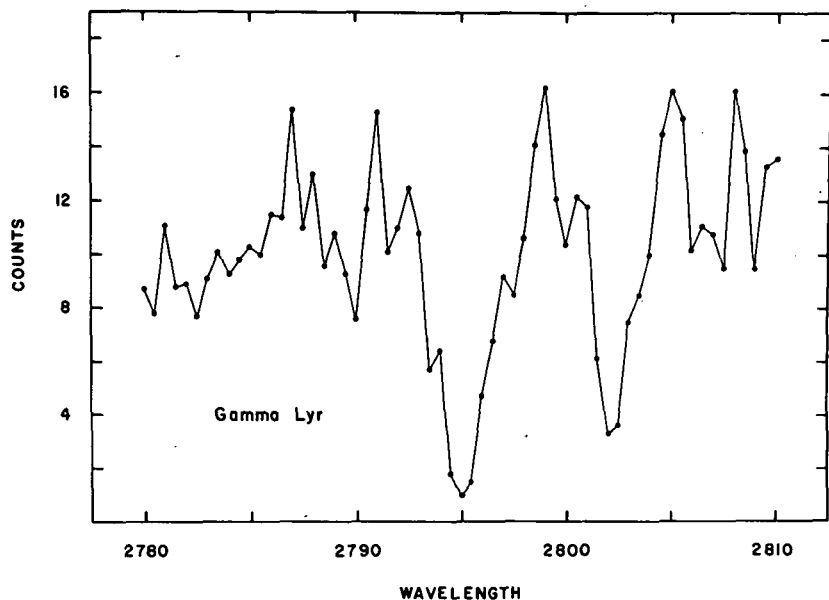


Figure II-11 Observation of the Mg II lines in $\gamma \text{ Lyr}$ on 1971 June 6/7.

The Mg II resonance doublet in γ Lyr appears as two deep, separated absorption lines. Correction for the stellar radial velocity of -22 km sec^{-1} (Hoffleit 1964) places the line centers at the observed absorption minima. The 2795 Å line is deeper and wider than the line at 2802 Å, as expected from the statistical weights. Although the exact continuum level is somewhat uncertain, the residual intensity in the bottom of the 2795 Å line appears to be about 0.1. There is no evidence for any emission associated with the Mg II lines in this star.

One objective of this project is to look for Mg II emission in early and mid F stars along the main sequence. Wilson (1966) studied rotational velocities and Ca II H and K emission along the main sequence between $b-y = 0.240$ and $b-y = 0.440$. He determined the regions of fast and slow rotation in the c_1 ($b-y$) diagram as shown in Figure II-12. Wilson found that the "fast rotation" region contained some slow rotators, while the "slow rotation" region contained no fast rotators. The boundary between the regions intersects the zero-age main sequence (ZAMS) near $b-y = 0.285$. Using 10 Å mm^{-1} Coude spectra, Wilson detected Ca II emission only as early as $b-y = 0.304$, although he suspected that higher-dispersion spectra might show Ca II emission as early as $b-y = 0.275$. We observed the Mg II resonance lines in the main-sequence F-stars β Cas and α CMi during the second flight. Both stars are plotted in Figure II-12 on the basis of the uv by photometry in the Stromgren-Perry Catalog (Stromgren and Perry 1965).

β Cas (F21V, $m_v = 2.2$) — Using the absolute magnitude calibration of Stromgren (1963), we find that β Cas is about $1^m.4$ above ZAMS. The Mg II resonance lines in β Cas (Figure II-13) appear as broad overlapping absorption lines with distinct minima. The 2795 Å line is deeper than the 2802 Å line. There is no prominent Mg II emission in this star. In order to investigate the existence of weak emission in the 2795 Å component we have smoothed the data over successively more channels in Figure II-14. The curves demonstrate that, even when the data are smoothed over 1 Å, the possible emission is still apparent. The stellar radial velocity is $+12 \text{ km sec}^{-1}$ (Hoffleit 1964). (Although β Cas is listed by Hoffleit (1964) as a spectroscopic binary, Abt (1970) finds no convincing evidence for this.) It is interesting to note that the low data points at 2795.5 Å are at the expected line center and might be a "K₃" component. The flat residual intensity which occurs in the bottom of the 2802 Å line may constitute weak emission at this wavelength.

α CMi (Procyon F51V, $m_v = 0.3$) — According to the Stromgren-Perry catalog photometry and Stromgren's (1963) calibration, Procyon is about $0^m.4$ above ZAMS. Procyon's $b-y$ value of 0.272 places it just outside Wilson's slow rotation region, but he classified it as a slow rotator. Kraft

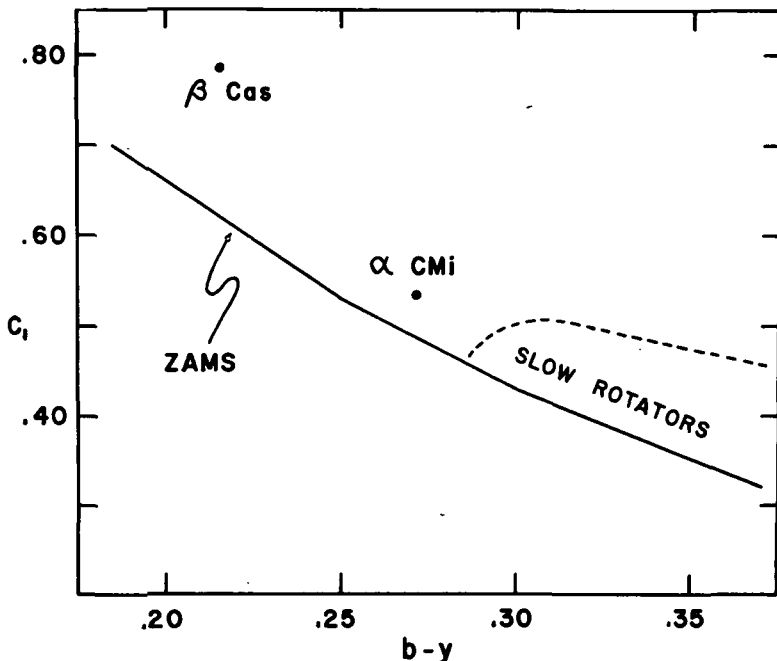


Figure II-12 c_1 -($b-y$) diagram for F stars. The solid line is Stromgren's (1963) Zero Age Main Sequence. The broken line is the boundary between Wilson's (1966) fast and slow rotation regions.

and Edmonds (1959) found "feeble but definitely present" Ca II emission in Procyon, using 3.2 and 4.8 \AA mm^{-1} spectra. They noted that the short-wavelength side of the emission appeared stronger than the long-wavelength side. Our microdensitometer tracing of the Coude plate of Procyon provided by O.C. Wilson (Figure II-15) also shows a similar weak Ca II K emission feature. Recently, Linsky (1972) observed similar K emission. Our Mg II observations of Procyon appear in Figure II-16. Procyon has a faint companion ($B\omega \Lambda 10$) with an orbital period of about 40 years. The γ velocity of the system is 4 km/sec and the semi-amplitude of the spectroscopic orbit is only 1.3 km/sec (Jones 1928). Thus the true Mg II line centers should be at $2795\frac{1}{2}$ and $2802\frac{3}{4} \text{ \AA}$. The most noticeable difference between the Procyon and β Cas Mg II lines is the distinct emission which appears in the Procyon lines. The emission feature at 2795 \AA is asymmetrical, with the stronger emission on the short-wavelength side, analogous to the Ca II observation in Procyon.

α Ori (Betelgeuse M2Iab, $m_v = 0.8v$) — Our Mg II observations of the supergiant α Ori are presented in Figure II-17. This shows both of the Mg

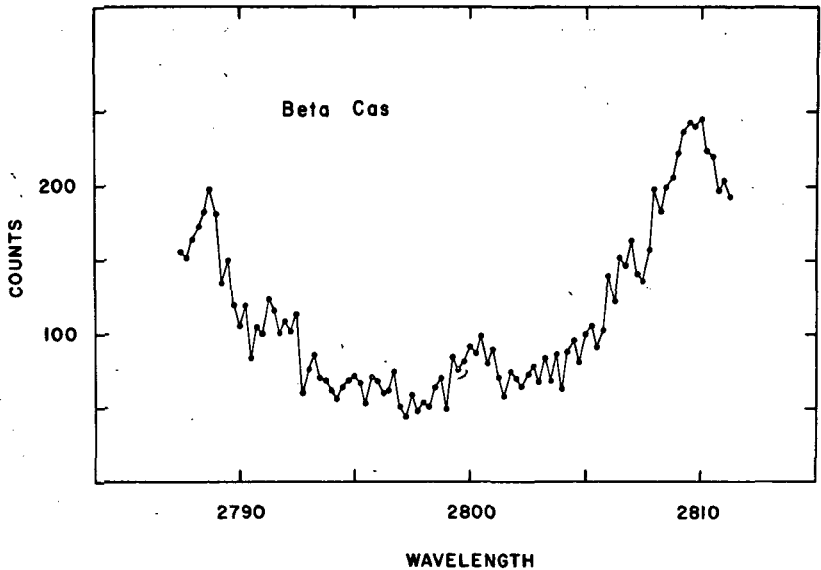


Figure II-13 Observation of the Mg II lines in β Cas on 1971 Oct. 7/8.

II resonance lines dramatically in emission, with each line showing prominent self-reversal. Figure II-18 shows a microdensitometer tracing of the vicinity of the Ca II K line in α Ori from a Coude plate loaned by O.C. Wilson. The Mg II emission is far more pronounced than the Ca II emission in this star.

The Mg II line centers corrected for the stellar radial velocity of + 21 km sec⁻¹ (Hoffleit 1964) should be located at 2795 $\frac{3}{4}$ and 2803.0 Å. The observed self-reversal minima are located at 2796.0 and 2803.5 Å. Considering our wavelength calibration uncertainty of $\pm \frac{1}{4}$ Å and our resolution of between 0.25 and 0.5 Å, it is not clear that the observed separation of the "K₃" and "H₃" minima is significant. We note that the "K₃" minimum in α Ori is deeper than the "H₃" minimum.

One of the striking features of the Mg II emission in α Ori is that the 2802 Å line is almost perfectly symmetric, while the 2795 Å line is definitely asymmetric. The height of the shorter-wavelength "K₂" peak is significantly lower than the height of the longer-wavelength "K₂" peak, although the "K₃" minimum is centered on the emission feature. Our planimetry of the two lines shows that the area under the 2802 Å line is about 12% greater than the area under the 2795 Å line. This difference in line shape between the 2795 and 2802 Å components is most puzzling. We are not sure how much of the count level outside the emission is true stellar continuum and how much is background count.

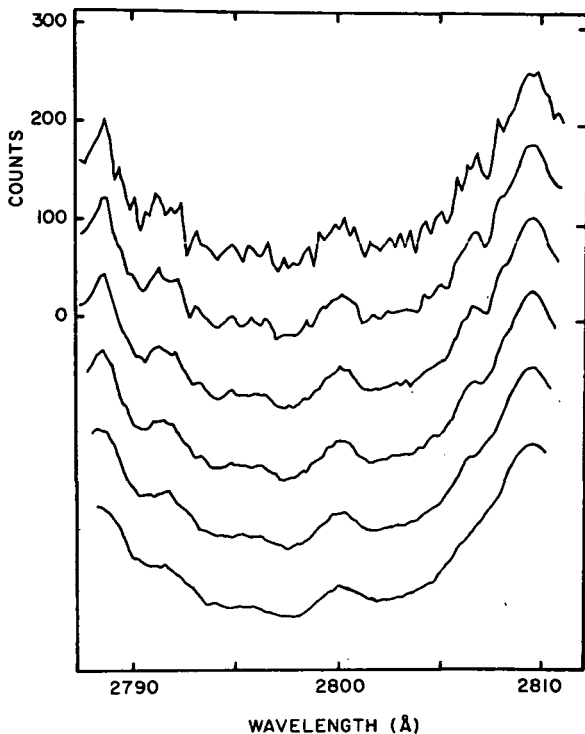


Figure II-14 The observation of the Mg II lines in β Cas smoothed successively over 1, 2, 3, 4, 6 and 8 channels.

We have measured the widths of both Mg II emission features in α Ori, the width of the 2795 Å emission in α CMi and the width of the possible 2795 Å emission in β Cas. We have also estimated the width of the 2795 Å emission in the solar spectrum from the published data of Purcell et al. (1961) and Lemaire (1970). Our estimates of the Mg II emission widths and their uncertainty are given in Table II-1.

TABLE II-1

Mg II Emission Widths		
Star	Width (Å)	Uncertainty (Å)
α Ori	3 3/4	$\pm 1/4$
β Cas	2 1/2	-1/4, +1/2
α CMi	1 1/2	-1/4, +1/2
Sun	0.7	± 0.1

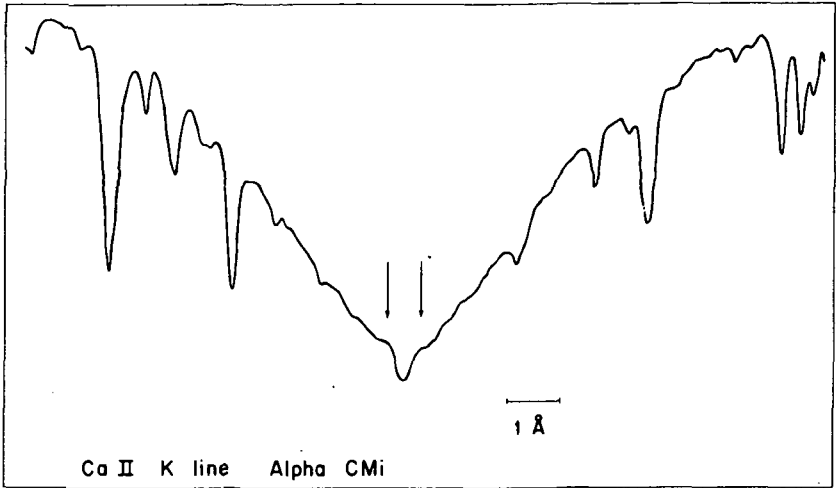


Figure II-15 Microdensitometer tracing of the Ca II K line in α CMi
The arrows indicate the K₂ peaks.

Figure II-19 is a plot of absolute visual magnitude versus $\text{Log } W$, where W is the full width of an emission line at its base in km sec^{-1} . This figure shows the Wilson-Bappu (1957) relationship between M_v and $\text{Log } W$ for Ca II K emission. On this figure we have superimposed our Mg II emission widths with error bars. Excluding β Cas, for which we are not certain that there is emission, we find that the Mg II emission widths are wider than the corresponding Ca II widths by $\Delta \log W \approx 0.4$. The present data are too limited to indicate definitely whether or not there is a unique relationship in this diagram from Mg II emission which is essentially independent of spectral type and emission strength, as is the case for Ca II.

The difference in width between the Ca II K and Mg II 2795 Å emission lines probably depends in part on the greater abundance of magnesium over calcium. However, it may also depend on the heights at which these "collision-controlled" lines are formed. The higher excitation and ionization potentials of magnesium provides an argument for Mg II lines being predominately formed at higher temperature and hence higher altitudes in the stellar chromosphere. An additional argument for Mg II line formation at higher altitudes is the increased optical thickness of the line due to the greater magnesium abundance. If the lines are formed at higher altitudes, then either increased turbulence, Doppler spreading due to a progressive increase in the radial flow velocity (if there is a stellar wind), or diffusion

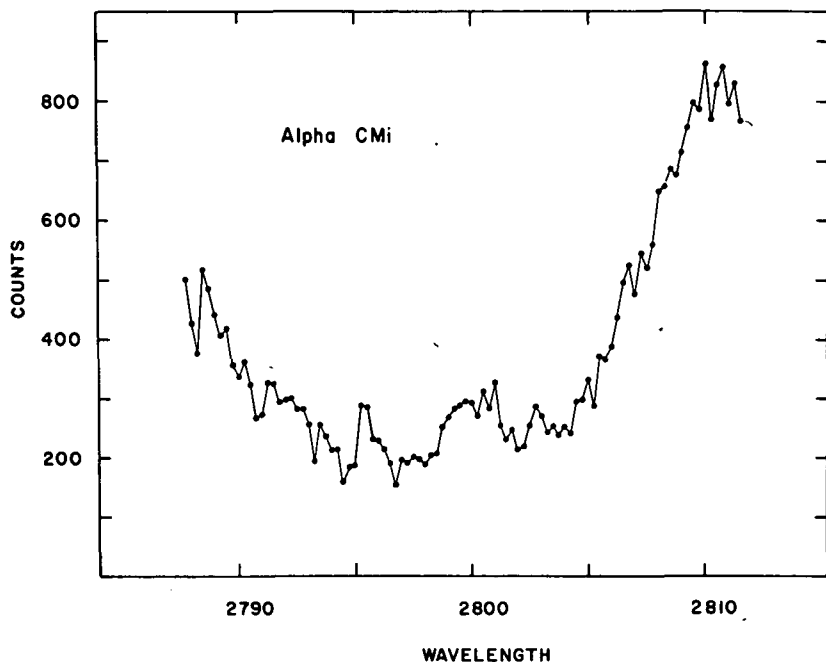


Figure II-16 Observation of the Mg II lines in α CMi on 1971 Oct. 7&8.

of the photons in wavelength for an optically thick line center could work to increase the line width.

We wish to thank the many people who supported us in the design, fabrication, testing, and flight support of the instrument. Finally, we would like to thank Dr. O.C. Wilson for making available his ground based Coude plates for comparison with our balloon observations.

REFERENCES

- Abt, H.A. 1962, *Ap. J.* 135, 424.
 . 1970, *Ap. J. Suppl.* 19, 387.
 Doherty, L.R. 1971, *Phil. Trans. Roy. Soc. Lon.* A270, 189.
 Gibson, W.C., Guthals, D.L., Jensen, J.W. and Eccher, J.A. 1972, submitted to *Rev. Sci. Instr.*
 Goldberg, L. 1954, *The Solar System*, II, G.P. Kuiper, ed. (Chicago: University of Chicago Press), p. 434.
 Hoffleit, D. 1964, *Catalogue of Bright Stars* (New Haven: Yale University Observatory).

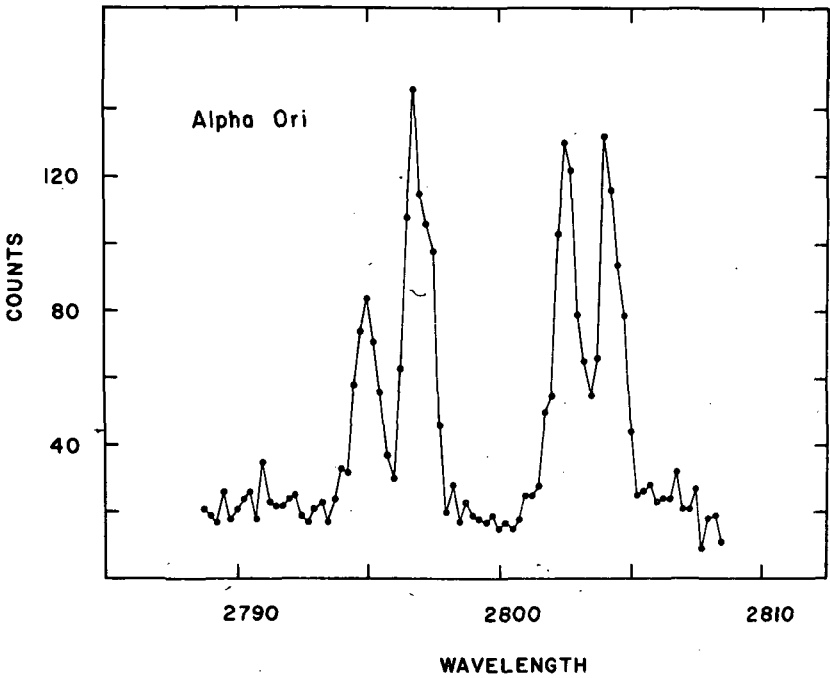


Figure II-17 Observation of the Mg II lines in α Ori on 1971 Oct. 7/8.

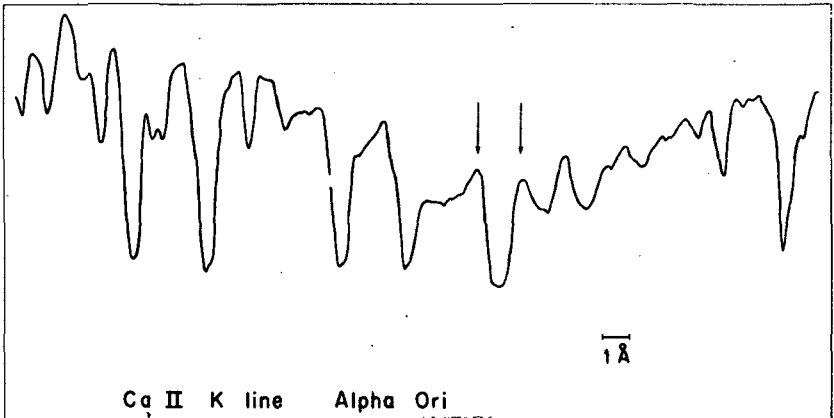


Figure II-18 Microdensitometer tracing of the Ca II K line in α Ori.
The arrows indicate the K_2 peaks.

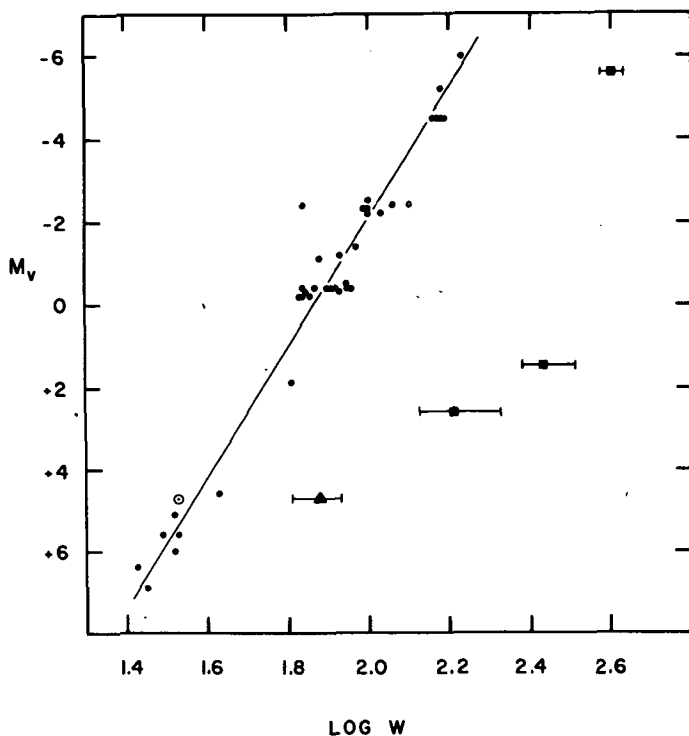


Figure II-19 Plot of M_v versus $\text{Log } (W)$, where W is the width of an emission line in km sec^{-1} . The filled circles are Ca II widths from Wilson and Bappu (1957). The dotted circle is the Ca II width in the Sun (Wilson and Bappu 1957). The squares are Mg II widths in α Ori, β Cas and α CMi respectively, in order of decreasing luminosity. The triangle is the solar Mg II width.

Jones, H.S. 1928, *M.N.R.A.S.* 88, 403.

Kondo, Y. 1972, *Ap.J.* 171, 605.

Kondo, Y., Giuli, R.T., Modisette, J.L. and Rydgren, A.E. 1972, submitted to *Ap.J.*

Kraft, R.P. and Edmonds, F.N. Jr. 1959, *Ap. J.* 129, 522.

Lemaire, P. 1970, in *Ultraviolet Stellar Spectra and Related Ground-based Observations*; L. Houziaux and H.E. Butler, ed. (Dordrecht: D. Reidel Pub. Co.), p. 250.

Linsky, J.L. 1972, *IAU Colloquium No. 19*, in press.

Purcell, J.D., Boggess, A. III and Tousey, R. 1961, *Ann. Intern. Geophys. Year 12*, Part II, 627.

Stromgren, B. 1963, *Basic Astronomical Data*, K. Aa Strand, ed. (Chicago: University of Chicago Press), p. 123.

- Stromgren, G. and Perry, C.L. 1965, *Photoelectric uvby Photometry for 1217 Stars Brighter than 6m.5*, unpublished.
- Wells, C.W., Bottema, M. and Ray, A.J. 1972, submitted to *Applied Optics*.
- Wilson, O.C. and Bappu, M.K.V. 1957, *Ap.J.* 125, 661.
- Wilson, O.C. 1966, *Ap.J.* 144, 695.
- Wood, D.B. and Forbes, J.E. 1963, *A.J.* 68, 257.

CONTINUATION OF DISCUSSIONS FOLLOWING TALKS BY PRADERIE AND DOHERTY

Kuhi – Now let's have a general discussion of Francoise Praderie's paper. Let's first discuss the question of what we do mean by a chromosphere from an observational point of view. One thing that bothers me a great deal is the distinction between a stellar chromosphere as we've come to think of it in the Sun and the changes that seem to take place as one goes from cool stars like the Sun to hotter and hotter stars in which the distinction between the defining characteristics becomes ever more vague, in separating out a chromosphere, an extended atmosphere, an extended envelope, and so on.

Aller – I think it is very important to make, as you say, a distinction between a chromosphere on the one hand, and what have loosely been called extended envelopes and shells on the other. There are a number of objects in which the gradation from one to the other is certainly not clear cut. A good example is RR Telescopii. In that star you see a spectrum of ionized titanium and iron that looks qualitatively somewhat like the flash spectrum of the Sun. Superimposed on it, however, are increasingly higher levels of excitation; both forbidden and permitted iron lines, ranging on up from [Fe II] to [Fe VII]. In fact, [Fe VII] supplies the strongest features in the emission spectrum of this object. In looking at the spectrum carefully there seems to be no place where you can say everything of one or two levels of ionization should be assigned to an ordinary chromosphere and everything else is to be attributed to something else. There seems to be a steady gradation in excitation. It's almost as though we were looking at the solar spectrum, in the near UV region.

Steinitz – I would like more clarification of the definition of a chromosphere. One of the necessary conditions was defined to be mass flux, and it wasn't clear whether the idea was mass loss, or accretion, or just mass motion. Also could you clarify what exactly is meant by non-radiative energy transfer? Should this include or exclude specifically convection?

Praderie – I did not want to include mass loss as such as a necessary condition for a chromosphere, because I have no clear evidence that the